

# Predictive Multiplicity in Probabilistic Classification

Jamelle Watson-Daniels<sup>\*1</sup>, David C. Parkes<sup>†1</sup>, and Berk Ustun<sup>‡2</sup>

<sup>1</sup>School of Engineering and Applied Sciences, Harvard University

<sup>2</sup>Halıcıoğlu Data Science Institute, UCSD

## Abstract

For a prediction task, there may exist multiple models that perform almost equally well. This multiplicity complicates how we typically develop and deploy machine learning models. We study how multiplicity affects predictions – i.e., *predictive multiplicity* – in probabilistic classification. We introduce new measures for this setting and present optimization-based methods to compute these measures for convex empirical risk minimization problems like logistic regression. We apply our methodology to gain insight into why predictive multiplicity arises. We study the incidence and prevalence of predictive multiplicity in real-world risk assessment tasks. Our results emphasize the need to report multiplicity more widely.

## 1 Introduction

When selecting a predictive model, we typically choose the “best” model that optimizes a metric of interest such as prediction error or accuracy. One assumption inherent in this process is that similar models assign similar predictions. We challenge this assumption by measuring *predictive multiplicity* – how predictions change across *competing* models that perform almost equally well. We introduce methods to measure predictive multiplicity for probabilistic classification. For a given prediction task, we ask how often competing models assign predictions that conflict with the baseline.

Measuring predictive multiplicity in this setting is particularly important as probabilistic classification is increasingly incorporated into real-world risk assessment tasks. In healthcare, models assign risk estimates that inform treatment decisions [30, 38, 22]. In consumer finance, lenders use risk estimates to underwrite loans [3, 5]. In criminal justice, models assign risk estimates that guide sentencing and parole decisions [4, 25]. Understanding the sensitivity of individual risk estimates could help decision makers discount or disregard a given risk prediction and rely instead on human intuition or domain expertise. If we find that predictive multiplicity is prevalent for a model informing high-stakes decisions, it may be necessary to forego deployment and/or revisit past decisions informed by the model. Further, analyzing predictive multiplicity promotes accountability on the part of model developers, by considering whether individual risk estimates are reliable or vary widely based on the particular choice of model during training.

Despite its implications, predictive multiplicity is understudied in machine learning. While recent work on predictive multiplicity focuses on binary classification tasks (making 0/1 predictions [28]), the methods do not extend to our setting. Researchers need new techniques that include instances

---

\*jwatsondaniels@g.harvard.edu

†parkes@eecs.harvard.edu

‡berk@ucsd.edu

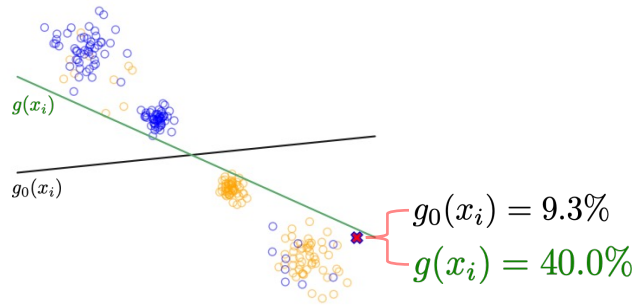


**Figure 1:** Classifiers that make the same binary predictions can still assign conflicting risk predictions. Here, we are given a 2D classification task with  $n^+ = 200$  positive examples (blue) and  $n^- = 200$  negative examples (orange). We plot the decision boundary of a baseline model  $g_0$  (black; log-loss/AUC/calibration = 0.41/0.88/17%) and a competing model  $g(x_i)$  (green) that performs almost equally well and makes the same binary predictions (log-loss/AUC/calibration = 0.42/0.89/16%). These classifiers assign wildly different risk estimates to individual examples; e.g., the predicted risk for the highlighted example is  $g_0(x_i) = 9.3\%$  but  $g(x_i) = 40.0\%$  under the competing model.

where there may not be conflicting predicted labels yet there are conflicting risk estimates (see Figure 1). For consistency in the literature, we expand the definitions in [28] to our setting. Whereas previous work only evaluates prediction variation over models with near-optimal loss, our methods enable developers to evaluate predictive multiplicity for additional near-optimal metrics.

The goal of this paper is to provide new methodology to study predictive multiplicity in probabilistic classification and to bring to the attention of practitioners the importance of measuring and reporting predictive multiplicity as a performance metric (similar to the universal measurement of test error).

Our main contributions are:

1. We formally define measures to report the prevalence of predictive multiplicity in probabilistic classification and develop new methodology to compute them, employing mixed-integer non-linear programming and outer-approximation algorithms.
2. To examine how risk predictions vary over competing models we define a new measure, the *viable prediction range*, and introduce an optimization-based method for computation.
3. We offer insights into why predictive multiplicity arises by conducting systematic experiments on synthetic data. We find that predictive multiplicity is more prevalent for examples that are both outliers and close to the discriminant boundary, for datasets that are less separable, and for minority groups when a dataset has a majority-minority structure.
4. We show that competing models can assign substantially different risk estimates and that a strikingly high proportion of examples are assigned conflicting estimates through an empirical study of seven real-world risk assessment tasks. Our results also demonstrate how multiplicity can disproportionately impact historically marginalized individuals, highlighting the social significance of developing methods to measure predictive multiplicity.

**Related Work.** Our work is broadly related to the research on the multiplicity of good models, and this effect has been occasionally referenced in the statistics literature [10, 9]. For example,

Chatfield [10] calls for performing a sensitivity analysis over competing models. Recent advances in computation have made it possible to perform these kinds of sensitivity analyses, leading to a stream of research on how competing models differ in terms of variable importance [16, 13], invariance to spurious correlations [11, 41], post-hoc explanations [33], and group fairness [1]. One way that we compute predictive multiplicity is by constructing a range of risk predictions for each example, these ranges are then used to quantify uncertainty in individual predictions. This relates to methods for evaluating predictive uncertainty such as conformal prediction [36, 34] as well as Bayesian approaches [see e.g., 14, 26]. However, conformal prediction focuses on uncertainty that arises due to non-conformity between historical data and new data, which is tangential to predictive multiplicity that arises from competing models on a single dataset sample. We focus on a non-Bayesian approach, recognizing that non-Bayesian methods are very typical in applied machine learning pipelines. Our goals relate also to a line of work that aims to quantify and communicate uncertainty in machine learning [18, 21, 29, 37, 24] and calibrate trust among stakeholders [20]. Other complementary work seeks interventions to resolve predictive multiplicity through model selection [1] or ensembling [8].

## 2 Framework

### 2.1 Preliminaries

We consider a probabilistic classification task with a dataset of  $n$  examples  $\mathcal{D} = \{(\mathbf{x}_i, y_i)\}_{i=1}^n$ . Each example consists of a feature vector  $\mathbf{x}_i = [1, x_{i1}, \dots, x_{id}] \in \mathcal{X} \subseteq \mathbb{R}^{d+1}$  and a label  $y_i \in \mathcal{Y} = \{-1, +1\}$ , where  $y_i = +1$  is an event of interest (e.g., default on a loan). With the dataset, we train a probabilistic classifier  $g : \mathcal{X} \rightarrow [0, 1]$  – i.e., a model that assigns a risk estimate to example  $\mathbf{x}_i$  as:  $g(\mathbf{x}_i) := \Pr(y_i = +1 | \mathbf{x}_i)$ . We refer to this model as the *baseline model*,  $g_0$ , because it is the optimal solution to an empirical risk minimization (ERM) problem of the form:

$$\min_{g \in \mathcal{H}} L(g; \mathcal{D}), \quad (1)$$

where  $\mathcal{H}$  is a family of probabilistic classifiers, and  $L(\cdot; \mathcal{D})$  is a loss function evaluated on the dataset  $\mathcal{D}$ . In what follows, we write  $L(g)$  instead of  $L(g; \mathcal{D})$  for conciseness. We evaluate the performance of a model in terms of  $L(g)$ , as well as the following metrics:

1. *Risk Calibration*: A model with good risk calibration assigns risk predictions that match observed frequencies [32]. We measure risk calibration in terms of *expected calibration error*:

$$\text{ECE}(g) = \sum_{b=1}^B \frac{n_b}{n} |\hat{p}_b(g) - \bar{p}_b|. \quad (2)$$

Here:  $I_b$  is the index set of  $n_b$  examples in bin  $b \in [B]$ ; and  $\hat{p}_b(g) := \frac{1}{n_b} \sum_{i \in I_b} g(\mathbf{x}_i)$  and  $\bar{p}_b = \frac{1}{n_b} \sum_{i \in I_b} \mathbb{1}[y_i = +1]$  are the mean predicted risk and mean observed risk of examples in bin  $b \in [B]$ , respectively.

2. *Rank Accuracy*: A rank-accurate model outputs risk predictions that can be used to correctly order examples in terms of true risk. We assess rank accuracy using the *area under the ROC*

curve:

$$\text{AUC}(g) = \frac{1}{n^+n^-} \sum_{\substack{i:y_i=+1 \\ k:y_k=-1}} \mathbb{1}[g(\mathbf{x}_i) > g(\mathbf{x}_k)], \quad (3)$$

where  $n^+ = |\{i : y_i = +1\}|$  and  $n^- = |\{i : y_i = -1\}|$ .

In what follows, we let  $M(g; \mathcal{D}) \in \mathbb{R}_+$  denote the performance of  $g \in \mathcal{H}$  over a dataset  $\mathcal{D}$  in regard to *performance metric*  $M(g)$ , where the convention is that lower values of  $M(g)$  are better; when working with AUC, we measure the *AUC error*:  $M(g) = 1 - \text{AUC}(g)$ .

## 2.2 Competing Models

Competing models are classifiers with near-optimal performance compared to the baseline model. A *competing model* is any model  $g \in \mathcal{H}$  whose performance is within  $\epsilon$  of the baseline model  $g_0$ .

**Definition 1 ( $\epsilon$ -Level Set)** *Given a baseline model  $g_0$ , metric  $M$ , and error tolerance  $\epsilon > 0$ , the set of competing models ( $\epsilon$ -level set) is the set:*

$$\mathcal{H}_\epsilon(g_0) := \{g \in \mathcal{H} : M(g) \leq M(g_0) + \epsilon\}.$$

Our methods consider multiplicity over a range of  $\epsilon$  values. In practice, a suitable choice of  $\epsilon$  should reflect the epistemic uncertainty in the performance of the baseline model. For instance, one could employ bootstrap re-sampling to measure the model uncertainty due to sample variation or consider worst-case uncertainty through generalization bounds.

## 2.3 Measuring Viable Risk Predictions

To examine how multiplicity affects predictions, we define the range of viable risk estimates that are output by competing models.

**Definition 2 (Viable Prediction Range)** *The viable prediction range is the smallest and largest risk estimate assigned to example  $i$  over competing models in the  $\epsilon$ -level set:*

$$V_\epsilon(\mathbf{x}_i) := \left[ \min_{g \in \mathcal{H}_\epsilon(g_0)} g(\mathbf{x}_i), \max_{g \in \mathcal{H}_\epsilon(g_0)} g(\mathbf{x}_i) \right]. \quad (4)$$

For a prediction task, computing the viable prediction ranges over a sample illuminates the extent to which similarly performing models assign different risk estimates to individuals. Although we express the prediction range over an  $\epsilon$ -level set using  $[\cdot, \cdot]$  interval notation, not all predictions between the min and the max may be attainable by a competing model.

## 2.4 Measuring Predictive Multiplicity

We say that a risk estimate is *conflicting* if it differs from the baseline risk estimate by at least some deviation threshold,  $\delta$ . We consider a range of the deviation threshold,  $\delta \in (0, 1)$ , and the appropriate range to consider will depend on the application; i.e., a conflict in a clinical decision support task may differ from that which constitutes a conflict in recidivism prediction. The following examples illustrate the importance of reporting predictive multiplicity over a range of  $\delta$  values.

*Recidivism Prediction:* Consider the task of predicting an individual’s risk of failing to appear in court using past arrest data [26]. Suppose there are four risk categories partitioned as follows– low: 0-10%, medium-low: 10-20%, medium-high: 20-30%, high: 30-100%. In this example, a deviation threshold  $\delta = 10\%$  is informative because it corresponds to a risk assessment shift that would constitute a risk category change for any individual in the first three categories.

*Medical Risk Prediction:* Consider the task of predicting stroke risk for patients with atrial fibrillation (MDCalc.com). The individual risk estimates can be used to inform blood thinner prescription decisions. One recommended usage suggests the following partitioning– 0% - 0.3%: do not prescribe blood thinner, 0.3-2.8%: maybe prescribe blood thinner, 2.9%+: prescribe blood thinner. If we study predictive multiplicity for this model, a value such as  $\delta = 1\%$  is informative because a risk estimate shift by 1% could change the decision to prescribe a blood thinner for many individuals.

We define ambiguity and discrepancy to reflect the proportion of examples in a sample  $S$  assigned conflicting risk estimates by competing models. These definitions follow Marx et al. [28], who give analogous definitions for the problem of multiplicity with binary predictions (see Figure 1 for an illustration of the difference between this problem and the multiplicity of risk estimates).

**Definition 3 (Ambiguity)** *The  $(\epsilon, \delta)$ -ambiguity of a probabilistic classification task over a sample  $S$  is the proportion of examples in  $S$  whose baseline risk estimate changes by at least  $\delta$  over the  $\epsilon$ -level set:*

$$A_{\delta, \epsilon}(g_0; S) := \frac{1}{|S|} \sum_{i \in S} \mathbb{1}[\max_{g \in \mathcal{H}_\epsilon(g_0)} |g(\mathbf{x}_i) - g_0(\mathbf{x}_i)| \geq \delta]. \quad (5)$$

Relative to the baseline model, ambiguity makes a statement about the proportion of individuals whose risk estimate is uncertain by at least  $\delta$ . High ambiguity means more uncertainty in individual risk predictions. Users may also consult the viable prediction range to guide decisions using the baseline model.

**Definition 4 (Discrepancy)** *The  $(\epsilon, \delta)$ -discrepancy of a probabilistic classification task over a sample  $S$  is the maximum proportion of examples in  $S$  whose risk estimates could change by at least  $\delta$  by switching the baseline model with a competing model in the  $\epsilon$ -level set:*

$$D_{\delta, \epsilon}(g_0; S) := \max_{g \in \mathcal{H}_\epsilon(g_0)} \frac{1}{|S|} \sum_{i \in S} \mathbb{1}[|g(\mathbf{x}_i) - g_0(\mathbf{x}_i)| \geq \delta]. \quad (6)$$

Relative to the baseline model, discrepancy reflects the maximum the number of conflicting risk estimates as a result of replacing baseline model with a competing model in the  $\epsilon$ -level set.

Ambiguity and discrepancy differ in the stance they take in regard to the worst case. Discrepancy measures the worst-case number of predictions that will change by switching the baseline model with a competing model. In contrast, ambiguity focuses on the worst case for prediction variation over the set of competing models. If we think about ambiguity as representing inconsistent outcomes and employ selective methods [e.g., 8] that abstain from predicting on those individuals, ambiguity would reflect the abstention rate.

**Ambiguity Relates to Viable Prediction Range.** In addition to revealing how multiplicity affects prediction variation, the viable prediction range contains information directly related to

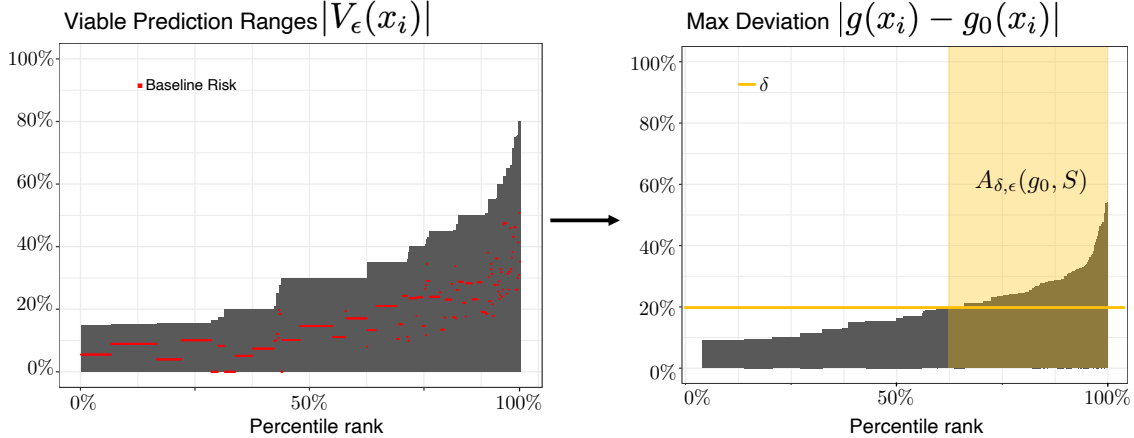


**Figure 2:** Illustration showing how the viable prediction range relates to ambiguity. Left, we plot the magnitude of the viable prediction range,  $V_\epsilon(\mathbf{x}_i)$  as well as the baseline risk estimate. From the viable prediction range, we can take the max difference from the baseline (right). Given a deviation threshold,  $\delta$ , the examples assigned conflicting risk estimates can be identified to compute ambiguity,  $A_{\delta, \epsilon}(g_0; S)$ , highlighted in yellow.

ambiguity. We illustrate this relationship in Figure 2. Given the viable prediction range for each example, we can calculate the maximum difference between the baseline risk and that assigned by competing models. We can then choose the deviation threshold  $\delta$  to determine which examples are assigned conflicting risk predictions, giving us ambiguity.

### 3 Methodology

In this section, we detail the procedure for computing measures of predictive multiplicity. This methodology can be applied to any convex loss function  $L(\cdot)$ , and together with a training problem that employs a convex regularization term. We illustrate the methodology on the classification task described in §2 by training a probabilistic classifier via logistic regression, with  $g(\mathbf{x}_i) = \frac{1}{1 + \exp(-\langle \mathbf{w}, \mathbf{x}_i \rangle)}$ , where  $\mathbf{w} = [w_0, w_1, \dots, w_d]^\top \in \mathbb{R}^{d+1}$  is a coefficient vector. We train this baseline model by solving Eq. (1) to minimize normalized *logistic loss*:  $L(\mathbf{w}) = \frac{1}{n} \sum_{i=1}^n \log(1 + \exp(-\langle \mathbf{w}, y_i \mathbf{x}_i \rangle))$ .

#### 3.1 Measuring Ambiguity

We first present a method for computing the ambiguity for different choices of  $\epsilon$  and  $\delta$ . The method also gives a conservative approximation of the viable prediction range for each example. We construct a pool of *candidate models* that assign a specific risk estimate to each example. From these models, we select those with performance within  $\epsilon$  of the baseline model as the set of competing models.

**Definition 5 (Candidate Model)** *Given a baseline model  $g_0$ , a finite set of user-specified threshold probabilities  $P \subseteq [0, 1]$ , then for each  $p \in P$  a candidate model for example  $\mathbf{x}_i$  is an optimal solution to the following constrained ERM:*

$$\begin{aligned}
 & \min_{\mathbf{w} \in \mathbb{R}^{d+1}} L(\mathbf{w}) \\
 & \text{s.t. } g(\mathbf{x}_i) \leq p, \quad \text{if } p < g_0(\mathbf{x}_i) \\
 & \quad \quad g(\mathbf{x}_i) \geq p, \quad \text{if } p > g_0(\mathbf{x}_i)
 \end{aligned} \tag{7}$$

For each threshold probability  $p \in P$ , we train a candidate model  $g$  such that the probability assigned to the example is constrained to the threshold  $p$ . In this way, by training for each example and threshold probability  $p \in P$ , we obtain the set of candidate models  $\mathcal{G} := \{g : i \in S, p \in P\}$ . We choose to solve the instances in order of increasing values of threshold probability  $p$ , which allows us to warm-start the optimization using previous solutions.

Given the set of candidate models, we define a *candidate  $\epsilon$ -level set* as

$$\tilde{\mathcal{H}}_\epsilon(g_0) = \{g \in \mathcal{G} : M(g) \leq M(g_0) + \epsilon\}. \quad (8)$$

We can use the candidate  $\epsilon$ -level set to compute measures of predictive multiplicity.

This method is exact for ambiguity defined in terms of near-optimal loss when the grid of threshold probabilities  $P \subseteq [0, 1]$  aligns with  $g_0(x_i) \pm \delta$  (i.e., is selected as appropriate to the baseline prediction for an example and the value of  $\delta$ ). For other metrics, such as AUC, this approach to compute ambiguity gives a conservative estimate (i.e., lower bound)—the training of a candidate model does not directly optimize for AUC, but we can retain only those candidate models that are competitive for the appropriate  $\epsilon$ -level set definition. Since  $\tilde{\mathcal{H}}_\epsilon(g_0) \subseteq \mathcal{H}_\epsilon(g_0)$ , the candidate-model approach also provides a conservative estimate of the viable prediction range (Eq. (4)) for an example.

### 3.2 Measuring Discrepancy

Discrepancy is the maximum proportion of examples assigned conflicting risk estimates by a single competing model,  $g \in \mathcal{H}_\epsilon(g_0)$ . Recall that a conflicting risk estimate differs from the baseline risk estimate  $g_0(\mathbf{x}_i)$  by at least some deviation threshold,  $\delta > 0$ . Therefore, measuring discrepancy with respect to a baseline model corresponds to solving the following maximization problem:

$$\max_{g \in \mathcal{H}_\epsilon(g_0)} \sum_{i \in S} \mathbb{1}[|g(\mathbf{x}_i) - g_0(\mathbf{x}_i)| \geq \delta]. \quad (9)$$

Given a sample  $S$ , the baseline loss  $L_0$ , error tolerance  $\epsilon$ , and deviation threshold  $\delta$ , we can formulate Eq. (9) as a mixed-integer non-linear program (MINLP):

$$\begin{aligned} \max_{\mathbf{w} \in \mathbb{R}^{d+1}} \quad & \sum_{i \in S} d_i \\ \text{s.t.} \quad & L(\mathbf{w}) \leq L_0 + \epsilon \end{aligned} \quad (10a)$$

$$d_i = v_{i,\delta} + z_{i,\delta} \quad \forall i \in S \quad (10b)$$

$$M_{z,i}(1 - z_{i,\delta}) \geq \langle \mathbf{w}, \mathbf{x}_i \rangle - U_{i,\delta} \quad \forall i \in S \quad (10c)$$

$$M_{v,i}(1 - v_{i,\delta}) \geq -\langle \mathbf{w}, \mathbf{x}_i \rangle + B_{i,\delta} \quad \forall i \in S \quad (10d)$$

$$d_i, z_{i,\delta}, v_{i,\delta} \in \{0, 1\} \quad \forall i \in S$$

The objective in Eq. (10) is the sum of examples assigned a conflicting risk estimates,  $d_i = \mathbb{1}[|g(\mathbf{x}_i) - g_0(\mathbf{x}_i)| \geq \delta]$ . The absolute value means  $d_i$  can be broken up into two indicator variables,  $d_i = \mathbb{1}[g(\mathbf{x}_i) \geq (\delta + g_0(\mathbf{x}_i))] + \mathbb{1}[g(\mathbf{x}_i) \leq (g_0(\mathbf{x}_i) - \delta)]$ . We introduce  $z_{i,\delta} = \mathbb{1}[g(\mathbf{x}_i) \leq (g_0(\mathbf{x}_i) - \delta)]$  and  $v_{i,\delta} = \mathbb{1}[g(\mathbf{x}_i) \geq (g_0(\mathbf{x}_i) + \delta)]$  to represent this behavior. Each  $d_i$  is set to  $z_{i,\delta}$  (or  $v_{i,\delta}$ ) when the model assigns a risk estimate to example  $i$  that exceeds  $\delta$  on the low-side (or high-side) of the baseline risk estimate, respectively. We ensure the indicator behavior of  $z_{i,\delta}$  and  $v_{i,\delta}$  through the ‘‘Big-M’’ constraints (10d) and (10c) whose parameters can be set as  $M_{z,i} := -U_{i,\delta} + \max_{\mathbf{w}} \langle \mathbf{w}, \mathbf{x}_i \rangle$  and  $M_{v,i} := B_{i,\delta} - \min_{\mathbf{w}} \langle \mathbf{w}, \mathbf{x}_i \rangle$ . For computation, we use score space and set the values of

$U_{i,\delta} := \text{logit}(g_0(\mathbf{x}_i) - \delta)$ , and  $B_{i,\delta} := \text{logit}(g_0(\mathbf{x}_i) + \delta)$ . When these quantities are outside of the  $[0, 1]$  domain of the logit, we can simply drop the relevant indicator variable from the formulation. We provide detailed derivations for our MINLP formulation in Appendix A.

**Outer-Approximation Algorithm.** The challenge in solving (10) is that constraint (10a) is non-linear. Therefore, we construct a linear approximation of the loss [see e.g., 17, 19] using an iterative, outer-approximation method [see e.g., 39, 7, 6] to solve. The algorithm recovers a globally optimal solution to the MINLP in (10) using a mixed-integer programming solver with callback functions [see e.g., 39, 7, 6]. The procedure builds a branch-and-bound tree to discover integer-feasible solutions that obey all constraints other than constraint (10a). For each feasible solution identified, it computes its loss to determine whether it is feasible with respect to constraint (10a). If feasible, this solution is retained. If not, it updates its approximation of the loss with the addition of a new linear constraint.

This method is exact for computing discrepancy in terms of near-optimal loss. For other metrics, we can again treat the intermediate solutions to the outer-approximation algorithm as candidate models and use these candidates to recover a lower bound for discrepancy similar to the method used in § 3.1.

## 4 Numerical Experiments

In this section, we present experiments on synthetic and real-world data. Our goal is two-fold: reveal data characteristics that impact predictive multiplicity, and determine the extent to which real risk assessment tasks exhibit predictive multiplicity in practice.

### 4.1 Properties that Influence Predictive Multiplicity

**Linear Separability.** To demonstrate how data separability informs predictive multiplicity, we compute ambiguity while varying the degree of separability and show results in Figure 3 column (A). We set  $\delta = 20\%$  and  $\epsilon = 5\%$  and control separability by increasing the variance of the data from  $\sigma = 4$  (top) to  $\sigma = 10$  (bottom). A clear trend is that ambiguity increases as the data becomes less separable from 1% to 21%. Notice, also that the ambiguous examples tend to be those near the discriminant boundary and outliers.

**Outliers and Margin Distance.** We examine how predictive multiplicity relates to outlier distance from the discriminant boundary. We position outliers near and far from the discriminant boundary and compute ambiguity. As shown in Figure 3 column (B), a clear trend is that examples that are outliers but far from the discriminant boundary (high margin) are less susceptible to predictive multiplicity.

**Majority-Minority Structure.** We consider the effect of systematically varying the majority-minority structure of a dataset. For this, we generate a majority class that has a different statistical pattern of features than a minority class. In the presence of the two groups, the model is faced with a tradeoff between correctly predicting one group or the other. In Figure 3 column (C), we vary the ratio in a majority-minority structure revealing that the minority group is more prone to



predictive multiplicity. The ambiguity of the minority group at 10:1 is substantially larger than for the majority group. This shows the importance of evaluating multiplicity across subgroups.

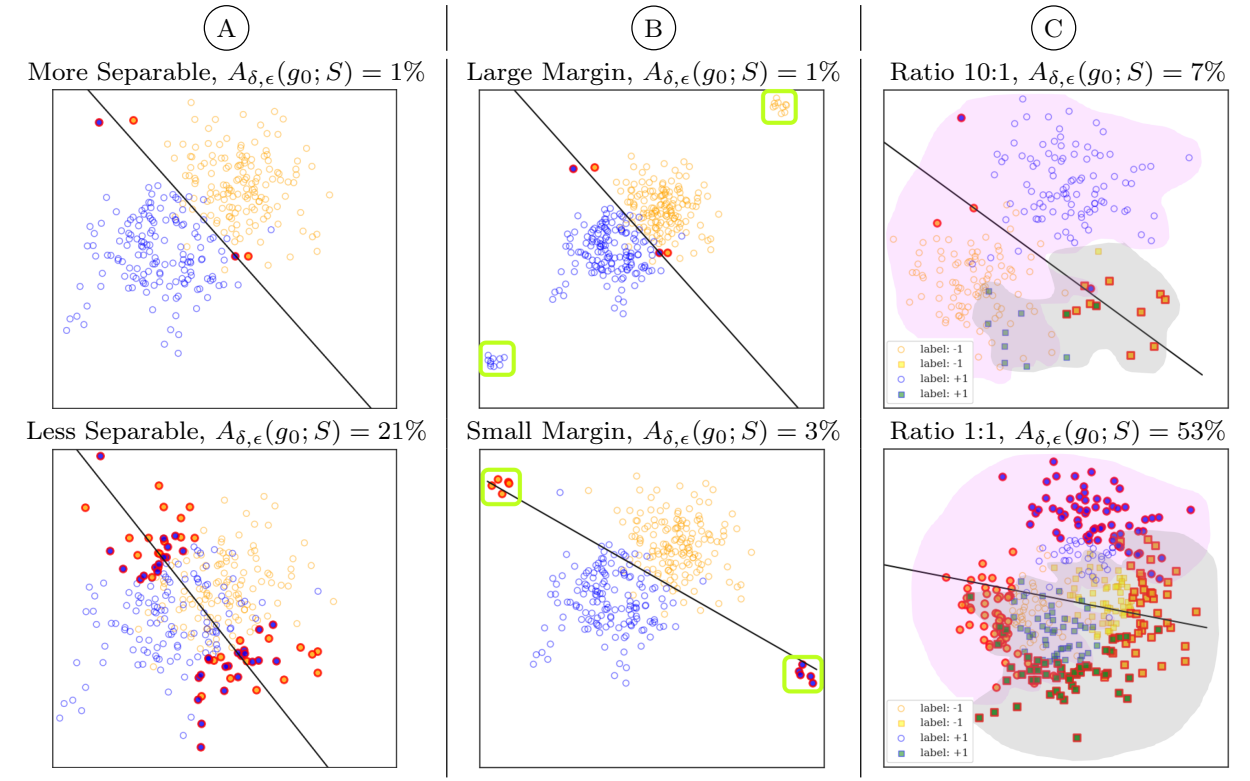


**Figure 3:** Experiments on synthetic data. In (A), we vary the degree of **separability** and find that ambiguity increases as separability decreases. In (B), we position **outliers** near and away from the discriminant boundary finding that outliers closer to the boundary are more prone to ambiguity. In (C), we vary the ratio in a **majority-minority** structured dataset: magenta shading- majority group (circles), grey shading- minority group (squares) revealing that the minority group is more prone to ambiguity. In the figures,  $Y = +1$  examples are blue,  $Y = -1$  examples are orange, and ambiguous examples are highlighted red and we set  $\delta = 20\%$  and  $\epsilon = 5\%$ .

## 4.2 Predictive Multiplicity in Risk Assessment Tasks

In this section, we evaluate predictive multiplicity in risk prediction tasks from medicine, lending, and criminal justice.<sup>1</sup> Altogether, we consider seven datasets that exhibit variations in sample size, number of features, and class imbalance (see Table 1 in the Appendix). For each dataset, we compute viable prediction ranges, ambiguity and discrepancy using the methods outlined in §3. When training candidate models, we adopt a grid of target predictions:  $P = \{0.01, 0.1, 0.2, \dots, 0.9, 0.99\}$ . We compute discrepancy by solving the MINLP Eq. (9) with CPLEX v20.1 [12] on a single CPU with 16GB RAM. Our results are shown in Figure 4, and additional results are in Appendix E.

**Viable Prediction Ranges.** Our results show that competing models can assign risk estimates that vary substantially. Viable prediction ranges are plotted in columns (A) and (B) of Figure 4,

<sup>1</sup>This is not an endorsement of current usage of risk assessment tools in criminal justice. The use of prediction software raises serious concerns in this domain. And we do not condone building models on arrest data to inform or justify increased policing.

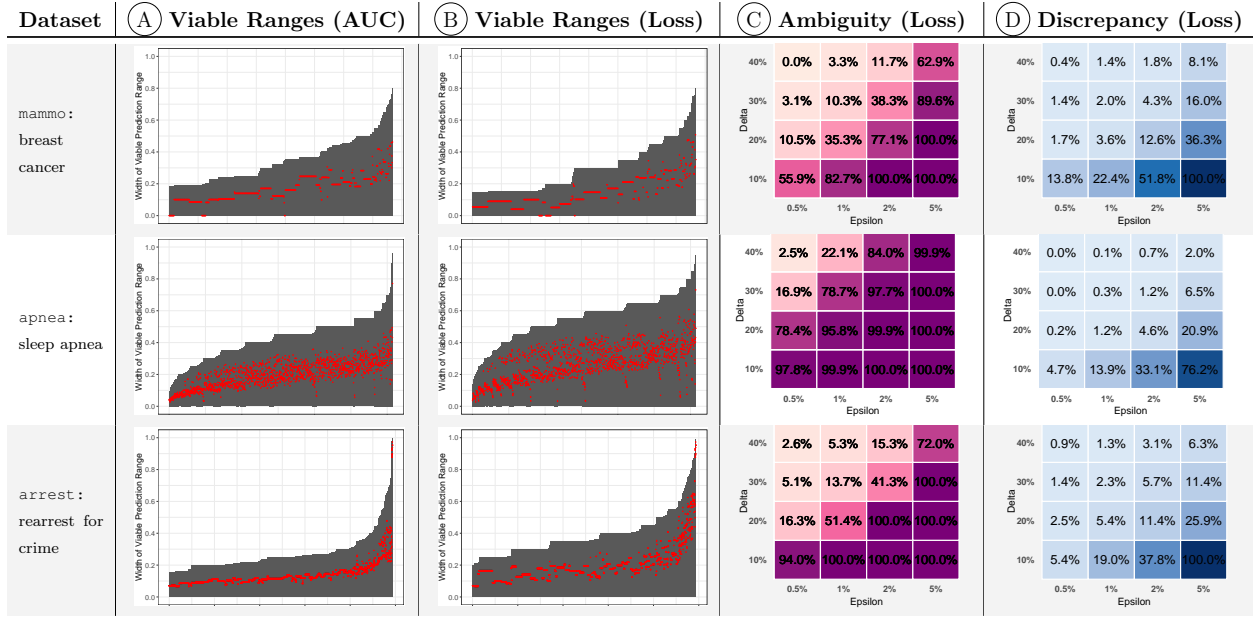


**Figure 4:** Predictive multiplicity in probabilistic classification on mammo, apnea and arrest. We show the distribution of viable prediction ranges ( $|V_\epsilon(\mathbf{x}_i)|$ ) on the y-axis, the x-axis percentile rank and relative baseline estimates in red) for competing models with near-optimal training AUC (A) and training loss (B). See illustration in Figure 2. We also show ambiguity (C) and discrepancy (D) for competing models with respect to training loss. We include similar results for the four other datasets in Appendix E.

and we see non-zero viable prediction ranges for all examples across all datasets. The viable ranges for apnea and mammo appear much larger compared to compas\_arrest. In terms of near-optimal loss, apnea has the most variation, while mammo has the most variation in terms of AUC. This points to the value in considering multiplicity for different near-optimal metrics.

**Ambiguity and Discrepancy.** Ambiguity and discrepancy are shown in columns (C) and (D) of Figure 4, respectively. For  $\epsilon = 1\%$  and  $\delta = 20\%$ , we see ambiguity values at 35.3% (mammo), 95.8% (apnea), and 51.4% (compas\_arrest). This means, for example, that 35.3% of breast cancer risk estimates vary by at least 20% over models within 1% optimal loss. We see discrepancy values at 3.6% (mammo), 1.2% (apnea), and 5.4% (compas\_arrest) for  $\epsilon = 1\%$  and  $\delta = 20\%$ . compas\_arrest is the worst in terms of discrepancy, while apnea has the most severe ambiguity. Thus, ambiguity and discrepancy are not always coupled.

**On the Choice of Performance Metric.** Our results show that the prevalence of predictive multiplicity depends on choice of near-optimal metric. In particular, we see that the distribution of viable predictions changes when we consider competing models in terms of AUC or loss. These differences translate into differences in summary statistics such as ambiguity and discrepancy: on the mammo dataset, ambiguity = 45% for 0.5% AUC and ambiguity = 35% for 1% loss ( $\delta = 20\%$ ). Likewise, for apnea, ambiguity = 79% for 0.5% AUC and ambiguity = 95% for 1% loss ( $\delta = 20\%$ ). This emphasizes the importance of methodology that allows for flexibility in regard to the choice of the metric for the near-optimality of a model.

**On Samples Prone to Ambiguity.** These experiments reveal a relationship between ambiguity and individual *uniqueness* (number of duplicates), *class* label, and *baseline risk estimate*. In terms of uniqueness, we find that across datasets, less than 10% of examples with more than 20 duplicates are ambiguous. That unique examples are more prone to ambiguity is related to our findings that outliers are often ambiguous (see §4.1).

In terms of class label, we find that positive examples are more likely to be ambiguous for datasets with class imbalance skewed negative, such as `adult` and `bank`. In comparison, datasets are roughly balanced by class (e.g., `mammo` and `compas_arrest`) have fairly balanced levels of ambiguity by class. This can be interpreted in light of the majority-minority effect from §4.1.

Lastly, and in terms of the baseline risk estimate, we see high ambiguity for examples with baseline risk near 50% on all datasets. For instance, 100% of examples with baseline risk between 45% and 55% are ambiguous for the `mammo` dataset ( $\epsilon = 0.5\%$  AUC,  $\delta = 20\%$ ). There is no reason to believe that high ambiguity is less problematic for these samples. Rather, the importance of ambiguity will depend on the risk thresholds that drive decisions in a particular domain.

**On the Disparate Impact of Multiplicity.** Given the real-life implications of individual risk prediction tasks, our results demonstrate how multiplicity can disproportionately impact individuals from historically marginalized backgrounds. For predicting the risk of rearrest, for example, our results show that individuals who are ethnically Hispanic are disproportionately affected by predictive multiplicity: the proportion of individuals assigned conflicting risk estimates is 39% for African Americans and 49% for Caucasians, compared to 98% for Hispanics ( $\epsilon = 1\%$  and  $\delta = 20\%$ ). Reporting predictive multiplicity for subgroups can reveal important ethical considerations when testing risk assessment models deployed throughout society.

## 5 Concluding Remarks

We develop methods to evaluate the effect of slightly perturbing optimal model performance, revealing that similar models do not always assign similar predictions. We propose a new framework for measuring predictive multiplicity for probabilistic classification through metrics (viable prediction range, ambiguity, discrepancy) and optimization-based methods to compute them. This includes detailed derivations, formulating a mixed-integer-non-linear program and an iterative, outer-approximation method to compute discrepancy.

Using synthetic data, we present the first study providing insight into the kinds of data characteristics that give rise to predictive multiplicity and show that separability, outliers and majority-minority structure are related to predictive multiplicity. Applied to seven datasets, we reveal concerning levels of predictive multiplicity in these high-stakes domains. More research is needed to examine predictive multiplicity for other loss functions (our methodology immediately generalizes to other convex loss functions) and to extend to other model classes. In future work, it will also be important to explore how to effectively communicate these effects to practitioners.

Our findings emphasize the importance of developing methods to measure and report predictive multiplicity. With information about how individual risk estimates change over competing models, we hope practitioners can make better decisions about how, and when, to rely on a model and when to make use of domain knowledge and human expertise in its place. Moreover, if there are particular kinds of individuals who are vulnerable to higher levels of predictive risk uncertainty, then we see reporting predictive multiplicity as promoting accountability for deployed models.

## References

- [1] Ali, J., Lahoti, P., and Gummadi, K. P. *Accounting for Model Uncertainty in Algorithmic Discrimination*, volume 1. Association for Computing Machinery, 2021. ISBN 9781450384735. doi: 10.1145/3461702.3462630.
- [2] Angwin, J., Larson, J., Mattu, S., and Kirchner, L. Machine Bias — ProPublica, 2016. URL <https://www.propublica.org/article/machine-bias-risk-assessments-in-criminal-sentencing>.
- [3] Attigeri, G. V., Pai, M. M., and Pai, R. M. Credit risk assessment using machine learning algorithms. *Advanced Science Letters*, 23(4):3649–3653, 2017. ISSN 19367317. doi: 10.1166/asl.2017.9018.
- [4] Austin, J., Ocker, R., and Bhati, A. Kentucky Pretrial Risk Assessment Instrument Validation. *The JFA Institute*, 5, 2010.
- [5] Bekhet, H. A. and Eletter, S. F. K. Credit risk assessment model for Jordanian commercial banks: Neural scoring approach. *Review of Development Finance*, 4(1):20–28, 2014. ISSN 18799337. doi: 10.1016/j.rdf.2014.03.002. URL <http://dx.doi.org/10.1016/j.rdf.2014.03.002>.
- [6] Bertsimas, D. and King, A. Logistic regression: From art to science. *Statistical Science*, pp. 367–384, 2017.
- [7] Bertsimas, D., King, A., Mazumder, R., et al. Best subset selection via a modern optimization lens. *Annals of statistics*, 44(2):813–852, 2016.
- [8] Black, E., Leino, K., and Fredrikson, M. Selective Ensembles for Consistent Predictions. (NeurIPS):1–24, 2021. URL <http://arxiv.org/abs/2111.08230>.
- [9] Breiman, L. Statistical modeling: The two cultures. *Statistical Science*, 16(3):199–215, 2001. ISSN 08834237. doi: 10.1214/ss/1009213726.
- [10] Chatfield, C. Model Uncertainty, Data Mining and Statistical Inference. *Journal of the Royal Statistical Society. Series A (Statistics in Society)*, 158(3):419, 1995. ISSN 09641998. doi: 10.2307/2983440.
- [11] D’Amour, A., Heller, K., Moldovan, D., Adlam, B., Alipanahi, B., Beutel, A., Chen, C., Deaton, J., Eisenstein, J., Hoffman, M. D., Hormozdiari, F., Houlsby, N., Hou, S., Jerfel, G., Karthikesalingam, A., Lucic, M., Ma, Y., McLean, C., Mincu, D., Mitani, A., Montanari, A., Nado, Z., Natarajan, V., Nielson, C., Osborne, T. F., Raman, R., Ramasamy, K., Sayres, R., Schrouff, J., Seneviratne, M., Sequeira, S., Suresh, H., Veitch, V., Vladymyrov, M., Wang, X., Webster, K., Yadlowsky, S., Yun, T., Zhai, X., and Sculley, D. Underspecification presents challenges for credibility in modern machine learning. *arXiv*, 2020. ISSN 23318422.
- [12] Diamond, S. and Boyd, S. CVXPY: A Python-embedded modeling language for convex optimization. *Journal of Machine Learning Research*, 17:1–5, 2016. ISSN 15337928.
- [13] Dong, J. and Rudin, C. Variable Importance Clouds: A Way to Explore Variable Importance for the Set of Good Models. 2019. URL <http://arxiv.org/abs/1901.03209>.

- [14] Dusenberry, M. W., Tran, D., Choi, E., Kemp, J., Nixon, J., Jerfel, G., Heller, K., and Dai, A. M. Analyzing the role of model uncertainty for electronic health records. *ACM CHIL 2020 - Proceedings of the 2020 ACM Conference on Health, Inference, and Learning*, pp. 204–213, 2020. doi: 10.1145/3368555.3384457.
- [15] Elter, M., Schulz-Wendtland, R., and Wittenberg, T. The prediction of breast cancer biopsy outcomes using two CAD approaches that both emphasize an intelligible decision process. *Medical Physics*, 34(11):4164–4172, 2007. ISSN 00942405. doi: 10.1118/1.2786864.
- [16] Fisher, A., Rudin, C., and Dominici, F. All models are wrong, but many are useful: Learning a variable’s importance by studying an entire class of prediction models simultaneously. *Journal of Machine Learning Research*, 20(Vi), 2019. ISSN 15337928.
- [17] Franc, V. and Sonnenburg, S. Optimized cutting plane algorithm for support vector machines. In *Proceedings of the 25th International Conference on Machine Learning*, pp. 320–327. ACM, 2008.
- [18] Hofman, J. M., Goldstein, D. G., and Hullman, J. How Visualizing Inferential Uncertainty Can Mislead Readers about Treatment Effects in Scientific Results. *Conference on Human Factors in Computing Systems - Proceedings*, 2020. doi: 10.1145/3313831.3376454.
- [19] Joachims, T., Finley, T., and Yu, C.-N. J. Cutting-plane training of structural SVMs. *Machine Learning*, 77(1):27–59, 2009.
- [20] Joslyn, S. and LeClerc, J. Decisions With Uncertainty: The Glass Half Full. *Current Directions in Psychological Science*, 22(4):308–315, 2013. ISSN 14678721. doi: 10.1177/0963721413481473.
- [21] Kale, A., Kay, M., and Hullman, J. Visual Reasoning Strategies for Effect Size Judgments and Decisions. *IEEE Transactions on Visualization and Computer Graphics*, pp. 1–1, 2020. ISSN 1077-2626. doi: 10.1109/tvcg.2020.3030335.
- [22] Khand, A., Frost, F., Grainger, R., Fisher, M., Chew, P., Mullen, L., Patel, B., Obeidat, M., Albouaini, K., Dodd, J., Goldstein, S. A., Newby, L. K., Cyr, D. D., Neely, M., Lüscher, T. F., Brown, E. B., White, H. D., Ohman, E. M., Roe, M. T., Hamm, C. W., Six, A. J., Backus, B. E., and Kelder, J. C. Heart Score Value. *Netherlands Heart Journal*, 10(6):1–10, 2017. ISSN 1568-5888.
- [23] Kohavi, R. Scaling up the accuracy of NB classifier : a DT hybrid. *Kdd*, (Utgoff 1988):202–207, 1996.
- [24] Kompa, B., Snoek, J., and Beam, A. L. Second opinion needed: communicating uncertainty in medical machine learning. *npj Digital Medicine*, 4(1), 2021. ISSN 23986352. doi: 10.1038/s41746-020-00367-3. URL <http://dx.doi.org/10.1038/s41746-020-00367-3>.
- [25] Latessa, E. J., Lemke, R., Makarios, M., Smith, P., and Lowenkamp, C. T. The creation and validation of the ohio risk assessment system (ORAS). *Federal Probation*, 74(1):16–22, 2010. ISSN 00149128.
- [26] Lum, K., Dunson, D. B., and Johndrow, J. Closer than they appear: A Bayesian perspective on individual-level heterogeneity in risk assessment. 2021. URL <http://arxiv.org/abs/2102.01135>.

- [27] Mangasarian, O. L., Street, W. N., and Wolberg, W. H. Breast Cancer Diagnosis and Prognosis Via Linear Programming. *Operations Research*, 43(4):570–577, 1995. ISSN 0030-364X. doi: 10.1287/opre.43.4.570.
- [28] Marx, C., Calmon, F. P., and Ustun, B. Predictive multiplicity in classification, 2019.
- [29] McGrath, S., Mehta, P., Zytek, A., Lage, I., and Lakkaraju, H. When Does Uncertainty Matter?: Understanding the Impact of Predictive Uncertainty in ML Assisted Decision Making. 2020. URL <http://arxiv.org/abs/2011.06167>.
- [30] Moreno, R. P., Metnitz, P. G., Almeida, E., Jordan, B., Bauer, P., Campos, R. A., Iapichino, G., Edbrooke, D., Capuzzo, M., and Le Gall, J. R. SAPS 3 - From evaluation of the patient to evaluation of the intensive care unit. Part 2: Development of a prognostic model for hospital mortality at ICU admission. *Intensive Care Medicine*, 31(10):1345–1355, 2005. ISSN 03424642. doi: 10.1007/s00134-005-2763-5.
- [31] Moro, S., Cortez, P., and Rita, P. A data-driven approach to predict the success of bank telemarketing. *Decision Support Systems*, 62:22–31, 2014. ISSN 01679236. doi: 10.1016/j.dss.2014.03.001. URL <http://dx.doi.org/10.1016/j.dss.2014.03.001>.
- [32] Naeini, M. P., Cooper, G. F., and Hauskrecht, M. Binary classifier calibration using a Bayesian non-parametric approach. *SIAM International Conference on Data Mining 2015, SDM 2015*, pp. 208–216, 2015. doi: 10.1137/1.9781611974010.24.
- [33] Pawelczyk, M., Broelemann, K., and Kasneci, G. On counterfactual explanations under predictive multiplicity. *Proceedings of the 36th Conference on Uncertainty in Artificial Intelligence, UAI 2020*, 124:839–848, 2020.
- [34] Romano, Y., Barber, R. F., Sabatti, C., and Candès, E. With Malice Toward None: Assessing Uncertainty via Equalized Coverage. *Harvard Data Science Review*, pp. 1–14, 2020. doi: 10.1162/99608f92.03f00592.
- [35] Salvatier, J., Wiecki, T. V., and Fonnesbeck, C. Probabilistic programming in Python using PyMC3. *PeerJ Computer Science*, 2016(4):1–20, 2016. ISSN 23765992. doi: 10.7717/peerj-cs.55.
- [36] Shafer, G. and Vovk, V. A tutorial on conformal prediction. *Journal of Machine Learning Research*, 9:371–421, 2008. ISSN 15324435.
- [37] Soyer, E. and Hogarth, R. M. The illusion of predictability: How regression statistics mislead experts. *International Journal of Forecasting*, 28(3):695–711, 2012. ISSN 01692070. doi: 10.1016/j.ijforecast.2012.02.002. URL <http://dx.doi.org/10.1016/j.ijforecast.2012.02.002>.
- [38] Than, M., Flaws, D., Sanders, S., Doust, J., Glasziou, P., Kline, J., Aldous, S., Troughton, R., Reid, C., Parsonage, W. A., Frampton, C., Greenslade, J. H., Deely, J. M., Hess, E., Sadiq, A. B., Singleton, R., Shopland, R., Vercoe, L., Woolhouse-Williams, M., Ardagh, M., Bossuyt, P., Bannister, L., and Cullen, L. Development and validation of the emergency department assessment of chest pain score and 2h accelerated diagnostic protocol. *EMA - Emergency Medicine Australasia*, 26(1):34–44, 2014. ISSN 17426731. doi: 10.1111/1742-6723.12164.

- [39] Ustun, B. and Rudin, C. Optimized Risk Scores. In *Proceedings of the 23rd ACM SIGKDD International Conference on Knowledge Discovery and Data Mining*. ACM, 2017.
- [40] Ustun, B., Westover, M. B., Rudin, C., and Bianchi, M. T. Clinical prediction models for sleep apnea: The importance of medical history over symptoms. *Journal of Clinical Sleep Medicine*, 12(2):161–168, 2016. ISSN 15509397. doi: 10.5664/jcsm.5476.
- [41] Veitch, V., D’Amour, A., Yadlowsky, S., and Eisenstein, J. Counterfactual invariance to spurious correlations: Why and how to pass stress tests. *arXiv preprint arXiv:2106.00545*, 2021.
- [42] Yeh, I. C. and Lien, C. h. The comparisons of data mining techniques for the predictive accuracy of probability of default of credit card clients. *Expert Systems with Applications*, 36(2 PART 1):2473–2480, 2009. ISSN 09574174. doi: 10.1016/j.eswa.2007.12.020. URL <http://dx.doi.org/10.1016/j.eswa.2007.12.020>.

## A MIP formulation for discrepancy ERM

To train a competing model that optimizes discrepancy, we solve a maximization problem of the form:

$$\max_{g \in \mathcal{H}_\epsilon(g_0)} \sum_{i=1}^n d_i \quad (11)$$

Here,  $d_i = \mathbb{1}[|g(\mathbf{x}_i) - g_0(\mathbf{x}_i)| \leq \delta]$  can also be rewritten in terms of score  $d_i = \mathbb{1}[s_w(\mathbf{x}_i) \geq \text{logit}(\delta + g_0(\mathbf{x}_i))] + \mathbb{1}[s_w(\mathbf{x}_i) \leq \text{logit}(g_0(\mathbf{x}_i) - \delta)]$ . We recover the solution to (11) by solving the following integer program:

$$\begin{aligned} \max_{\mathbf{w} \in \mathbb{R}^{d+1}} \quad & \sum_{i=0}^n d_i \\ \text{s.t.} \quad & L(\mathbf{w}) \leq L(\mathbf{w}_0) + \epsilon \end{aligned} \quad (12a)$$

$$d_i = v_{i,\delta} + z_{i,\delta} \quad i = 1, \dots, n \quad (12b)$$

$$M_{z,i}(1 - z_{i,\delta}) \geq (s_w(\mathbf{x}_i) - U_{i,\delta}) \quad i = 1, \dots, n \quad (12c)$$

$$M_{v,i}(1 - v_{i,\delta}) \geq -(s_w(\mathbf{x}_i) - B_{i,\delta}) \quad i = 1, \dots, n \quad (12d)$$

$$s_w(\mathbf{x}_i) = \sum_{j=0}^d w_j x_{i,j} \quad i = 1, \dots, n \quad (12e)$$

$$d_i \in \{0, 1\} \quad i = 1, \dots, n \quad (12f)$$

$$z_{i,\delta} \in \{0, 1\} \quad i = 1, \dots, n \quad (12g)$$

$$v_{i,\delta} \in \{0, 1\} \quad i = 1, \dots, n \quad (12h)$$

$$w_j \in \mathbb{R} \quad j = 0, \dots, d \quad (12i)$$

Here:

- $L(\mathbf{w}_0) := \frac{1}{n} \sum_{i=1}^n \log(1 + \exp(-\langle \mathbf{w}_0, y_i \mathbf{x}_i \rangle))$  is the log-loss of the baseline classifier on the training data
- $\epsilon \geq 0$  is the loss tolerance (i.e., the maximum additional loss of any competing classifier)
- $U_{i,\delta}$  is a parameter that we set as  $U_{i,\delta} := \text{logit}(g_0(\mathbf{x}_i) - \delta)$
- $B_{i,\delta}$  is a parameter that we set as  $B_{i,\delta} := \text{logit}(g_0(\mathbf{x}_i) + \delta)$
- $M_{z,i}$  is a Big-M parameter that we set as  $M_{z,i} = -U_{i,\delta} + \max_{\mathbf{w}} \sum_{j=0}^d w_j x_{i,j}$
- $M_{v,i}$  is a Big-M parameter that we set as  $M_{v,i} = B_{i,\delta} - \min_{\mathbf{w}} \sum_{j=0}^d w_j x_{i,j}$
- $W^{\max}$  and  $W^{\min}$  are user-defined coefficient bounds

**Big-M Derivations** Recall that by definition,

$$g(\mathbf{x}_i) := \Pr(y_i = +1 | \mathbf{x}_i) = \frac{1}{1 + \exp(-\langle \mathbf{w}, \mathbf{x}_i \rangle)} \quad (13)$$



Therefore,  $s_w(\mathbf{x}) = \text{logit}(g(\mathbf{x}_i))$ . Our goal is to write the objective,  $|g(\mathbf{x}_i) - g_0(\mathbf{x}_i)| \geq \delta$ , in terms of score,  $s_w(\mathbf{x}_i)$ .

$$\begin{aligned}
d_i &= \mathbb{1}[|g(\mathbf{x}_i) - g_0(\mathbf{x}_i)| \geq \delta], \\
&= \mathbb{1}[g(\mathbf{x}_i) - g_0(\mathbf{x}_i) \geq \delta] + \mathbb{1}[g_0(\mathbf{x}_i) - g(\mathbf{x}_i) \geq \delta] \\
&= \mathbb{1}[g(\mathbf{x}_i) \geq \delta + g_0(\mathbf{x}_i)] + \mathbb{1}[-g(\mathbf{x}_i) \geq \delta - g_0(\mathbf{x}_i)] \\
&= \mathbb{1}[g(\mathbf{x}_i) \geq g_0(\mathbf{x}_i) + \delta] + \mathbb{1}[g(\mathbf{x}_i) \leq g_0(\mathbf{x}_i) - \delta]
\end{aligned}$$

Now we transform into score space

$$\begin{aligned}
&= \mathbb{1}[\text{logit}(g(\mathbf{x}_i)) \geq \text{logit}(g_0(\mathbf{x}_i) + \delta)] + \mathbb{1}[\text{logit}(g(\mathbf{x}_i)) \leq \text{logit}(g_0(\mathbf{x}_i) - \delta)] \\
&= \mathbb{1}[s_w(\mathbf{x}_i) \geq \text{logit}(g_0(\mathbf{x}_i) + \delta)] + \mathbb{1}[s_w(\mathbf{x}_i) \leq \text{logit}(g_0(\mathbf{x}_i) - \delta)]
\end{aligned}$$

Let  $U_{i,\delta} = \text{logit}(g_0(\mathbf{x}_i) - \delta)$  and  $B_{i,\delta} = \text{logit}(g_0(\mathbf{x}_i) + \delta)$ .

$$\begin{aligned}
&= \mathbb{1}[s_w(\mathbf{x}_i) \geq B_{i,\delta}] + \mathbb{1}[s_w(\mathbf{x}_i) \leq U_{i,\delta}] \\
&= v_{i,\delta} + z_{i,\delta}
\end{aligned}$$

To ensure that  $z_{i,\delta} = 1$  whenever  $\mathbb{1}[s_w(\mathbf{x}_i) \leq U_{i,\delta}] = 1$ , and  $z_{i,\delta} = 0$  whenever  $\mathbb{1}[s_w(\mathbf{x}_i) \leq U_{i,\delta}] = 0$ , we add the following Big-M constraint:

$$M_{z,i}(1 - z_{i,\delta}) \geq s_w(\mathbf{x}_i) - U_{i,\delta}$$

Here we can set the Big-M parameter as:

$$\begin{aligned}
M_{z,i} &= \max_{\mathbf{w}}(s_w(\mathbf{x}_i) - U_{i,\delta}), \\
&= -U_{i,\delta} + \max_{\mathbf{w}} s_w(\mathbf{x}_i), \\
&= -U_{i,\delta} + \max_{\mathbf{w}} \langle \mathbf{w}, \mathbf{x}_i \rangle, \\
&= -U_{i,\delta} + \max_{\mathbf{w}} \sum_{j=0}^d w_j x_{ij} \\
&= -U_{i,\delta} + W^{\max} \sum_{j=0}^d x_{ij}
\end{aligned}$$

Next, to ensure that  $v_{i,\delta} = 1$  whenever  $\mathbb{1}[s_w(\mathbf{x}_i) \geq B_{i,\delta}] = 1$ , and that  $v_{i,\delta} = 0$  whenever  $\mathbb{1}[s_w(\mathbf{x}_i) \geq B_{i,\delta}] = 0$ , we add the following Big-M constraint:

$$M_{v,i}(1 - v_{i,\delta}) \geq -(s_w(\mathbf{x}_i) - B_{i,\delta})$$

Here, we can set the Big-M parameter as:

$$\begin{aligned}
M_{v,i} &= \max_{\mathbf{w}} (B_{i,\delta} - s_w(\mathbf{x}_i)), \\
&= B_{i,\delta} + \max_{\mathbf{w}} -s_w(\mathbf{x}_i), \\
&= B_{i,\delta} - \min_{\mathbf{w}} s_w(\mathbf{x}_i), \\
&= B_{i,\delta} - \min_{\mathbf{w}} \langle \mathbf{w}, \mathbf{x}_i \rangle, \\
&= B_{i,\delta} - \min_{\mathbf{w}} \sum_{j=0}^d w_j x_{ij}, \\
&= B_{i,\delta} - W^{\min} \sum_{j=0}^d x_{ij}
\end{aligned}$$

When performing experiments using CPLEX software, we set the MIP gap = 0.0 and the time limit to 600 seconds.

## B Outer Approximation Algorithm

**Loss Callback Formulation** We let  $L_\epsilon^{\max} := L^0 + \epsilon$ . This allows us to write the loss constraint  $L(\mathbf{w}) \leq L^0 + \epsilon$  as follows.

$$L(\mathbf{w}) \leq L_\epsilon^{\max} \tag{14}$$

$$L(\mathbf{w}) - L_\epsilon^{\max} \leq 0 \tag{15}$$

$$c(\mathbf{w}) \leq 0 \tag{16}$$

We will present an algorithm where we approximate  $c(\cdot)$  by a linear approximation at a fixed point  $\mathbf{w}^k \in \mathbb{R}^d$ . The linear approximation has the form:

$$\hat{c}^k(\mathbf{w}) := c(\mathbf{w}^k) + \nabla L(\mathbf{w}^k)(\mathbf{w} - \mathbf{w}^k) \tag{17}$$

$$= c(\mathbf{w}^k) + \sum_{j=1}^d \nabla L(w_j^k)(w_j - w_j^k) \tag{18}$$

Recall that  $L(\mathbf{w}) = \frac{1}{n} \sum_{i=1}^n \log(1 + \exp(-\langle \mathbf{w}^k, y_i \mathbf{x}_i \rangle))$ . The derivative evaluated at  $\mathbf{w}^k$  is therefore,

$$\nabla_j L(w_j^k) = \frac{1}{n} \sum_{i=1}^n \nabla_j \log(1 + \exp(-\langle \mathbf{w}^k, y_i \mathbf{x}_i \rangle)) \tag{19}$$

$$= \frac{1}{n} \sum_{i=1}^n \left[ \frac{1}{1 + \exp(-\langle \mathbf{w}^k, y_i \mathbf{x}_i \rangle)} * \exp(-\langle \mathbf{w}^k, y_i \mathbf{x}_i \rangle) * -y_i \mathbf{x}_i \right] \tag{20}$$

To perform the outer approximation, we add the following loss cut if  $L(\mathbf{w}^k) - L_\epsilon^{\max} > 0$

$$0 \geq L(\mathbf{w}^k) - L_\epsilon^{\max} + \sum_{j=1}^d \nabla L(w_j^k)(w_j - w_j^k) \quad (21)$$

$$0 \geq L(\mathbf{w}^k) - L_\epsilon^{\max} + \sum_{j=1}^d \nabla L(w_j^k) * w_j - \sum_{j=1}^d \nabla L(w_j^k) * w_j^k \quad (22)$$

$$-\sum_{j=1}^d \nabla L(w_j^k) * w_j \geq L(\mathbf{w}^k) - L_\epsilon^{\max} - \sum_{j=1}^d \nabla L(w_j^k) * w_j^k \quad (23)$$

## C Bayesian Comparison

To illustrate briefly how our approach compares with Bayesian methods, we compute the maximum loss in the 90% credible region, and set the multiplicity loss tolerance  $\epsilon$  to that value. For a single example selected from the `breastcancer` dataset, we plot the viable prediction range and the posterior predictive for models within the loss tolerance. We see in Figure 5 that the viable prediction range is significantly wider than the Bayesian 90% credible region, highlighting a difference between the two frameworks.

For this demonstration, we consider a logistic regression model, along with normal priors for parameters; we adopt a Gaussian prior on parameters  $\mathbf{w}_j$ , and set the mean to 0. We assume weak information regarding the true values of the parameters by adopting a large variance,  $\mathbf{w}_j \sim N(0, 10000)$  for each parameter. The likelihood is

$$\mathcal{L}(\mathbf{w}) = \prod_{i=1}^n p(\mathbf{x}_i)^{y_i} (1 - p(\mathbf{x}_i))^{(1-y_i)}.$$

We use Metropolis-Hastings to sample from the posterior using the MAP as a starting point and with 50,000 samples and two chains. After sampling, a trace object is returned that contains samples from the posterior distribution. We use the PyMC3 Python package [35].

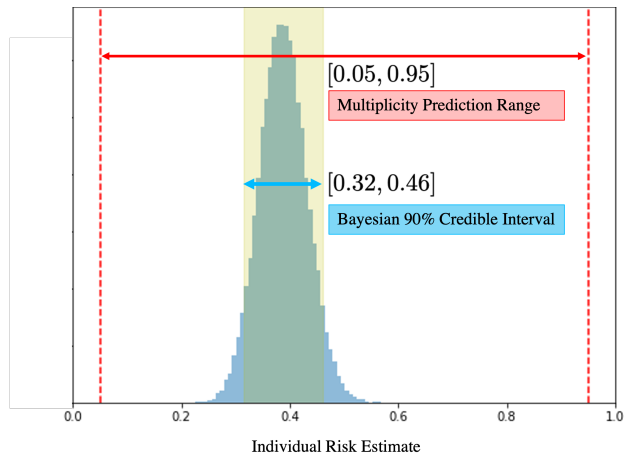


**Figure 5:** A comparison of a Bayesian 90% credible interval and the viable prediction range for a single example selected from a dataset. We perform this study on a small `breastcancer` dataset [27] for predicting whether patient breastcancer biopsy is malignant. Here, we compute the maximum loss in the 90% credible region, and set the multiplicity loss tolerance  $\epsilon$  to that value. The viable prediction range is substantially wider than the Bayesian 90% credible region, illustrating the difference between the two frameworks.

## D Datasets

Name	Outcome Variable	$n$	$d$	Class Imbalance	Train Loss	Train AUC	Train ECE
mammo [15]	mammogram shows breast cancer	961	12	0.86	0.471	85%	2.4%
credit [42]	customer default on loan	30,000	23	3.50	0.453	74%	1.6%
bank [31]	person opens bank account after marketing call	41,188	57	0.12	0.268	82%	0.9%
adult [23]	person in 1994 US census earns over \$50,000	32,561	36	0.31	0.332	90%	0.8%
compas_arrest [2]	rearrest for any crime	5,380	18	0.84	0.612	72%	1.1%
compas_violent [2]	rearrest for violent crime	8,768	18	0.13	0.332	67%	0.3%
apnea [40]	patient diagnosed with obstructive sleep apnea	1,537	36	0.70	0.565	76%	3.3%

**Table 1:** Publicly available datasets used to train risk assessment models in §4.2. For each dataset, we report  $n$ ,  $d$ , the class imbalance ratio,  $|n^+|/|n^-|$ , and the performance metrics of the baseline model on training data. We work with sub-sampled versions of `credit`, `bank` and `adult` by randomly sampling  $n = 5000$  points from each dataset.

### D.1 Synthetic Datasets

To study the causes of predictive multiplicity, we generate small, synthetic datasets to conduct the studies shown in Figure 3. For this, we generate isotropic Gaussian blobs for clustering, using sklearn functions. For the separability study, we generate a dataset with  $N = 200$  randomly generated samples with varying standard deviation. For the outliers study, we generate a dataset with  $N = 320$  randomly generated samples with two clusters of outliers at varied positions. For the majority-minority structure study, we generate a dataset with variation in  $N_{\text{majority}}$  and  $N_{\text{minority}}$ , with a complete population of size  $N = 150$  for each group, and this subsampled to lead to group imbalance.

## E Additional Results

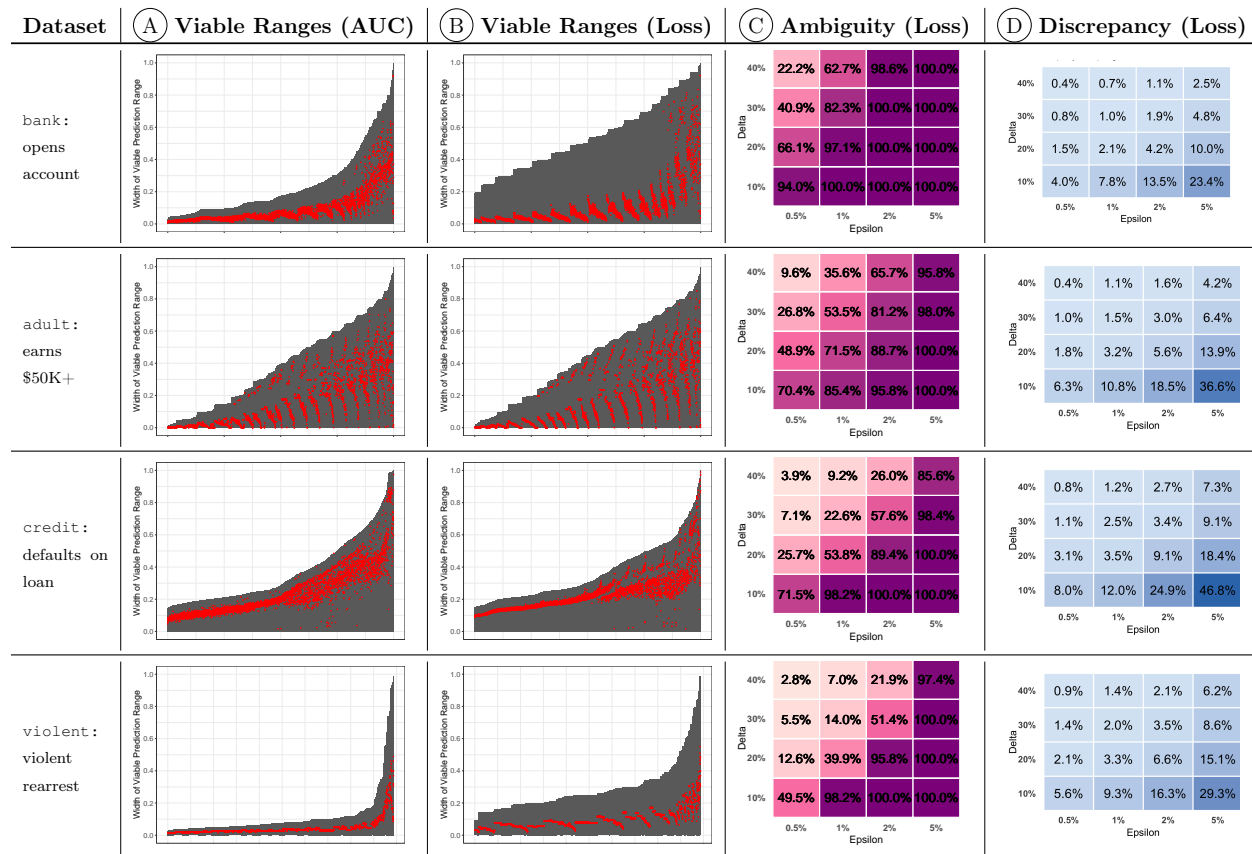


**Figure 6:** Predictive multiplicity in probabilistic classification on the additional datasets: bank, adult, credit and violent. We show the distribution of viable prediction ranges ( $|V_\epsilon(\mathbf{x}_i)|$  on the y-axis, the x-axis percentile rank and relative baseline estimates in red) for competing models with near-optimal training AUC (A) and training loss (B). See illustration in Figure 2. We also show ambiguity (C) and discrepancy (D) for competing models with respect to training loss.

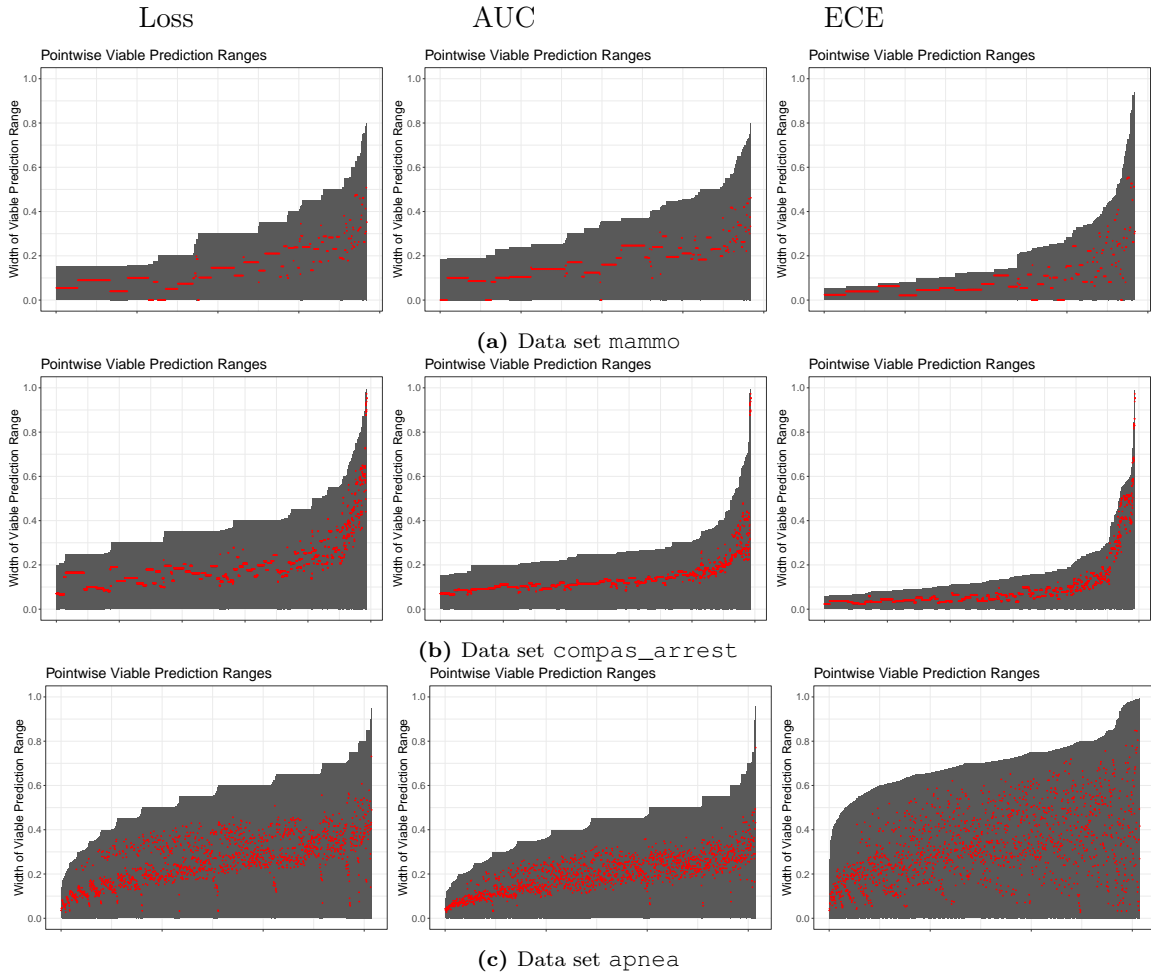
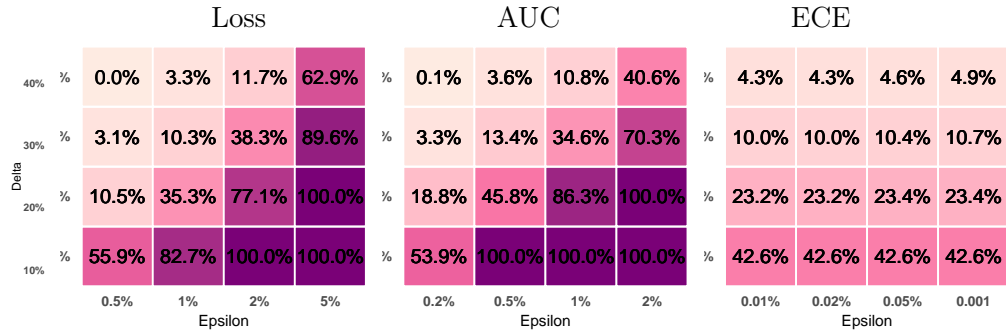
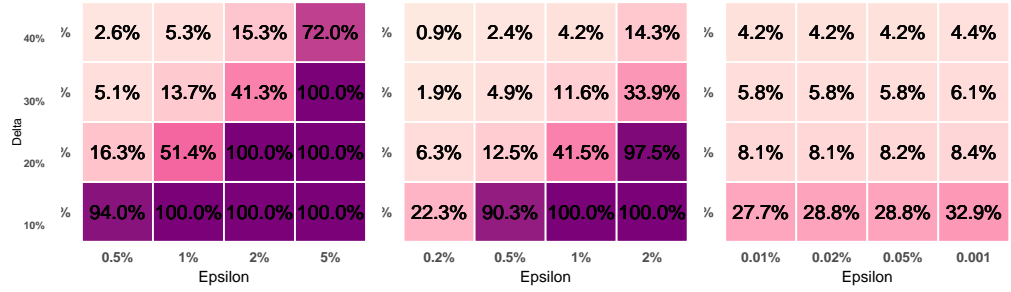


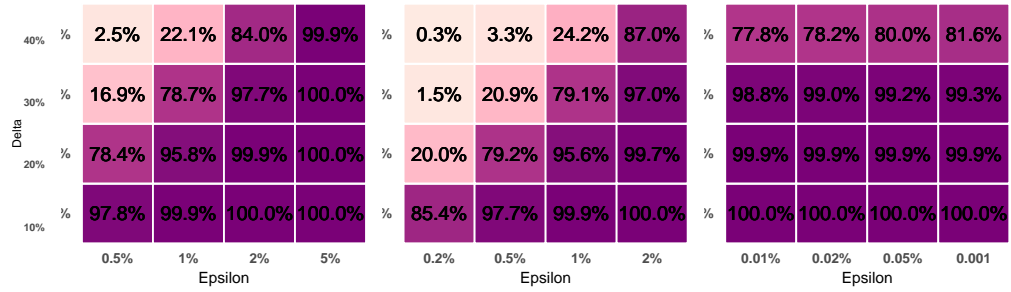
**Figure 7:** Additional viable prediction ranges ( $|V_\epsilon(\mathbf{x}_i)|$ ) for each near-optimal metric. Results shown for the datasets mammo, compas\_arrest, apnea, and for  $\epsilon$ -level sets defined on loss (1%), AUC (0.5%), and ECE (0.02%).



(a) Data set mammo



(b) Data set compas\_arrest



(c) Data set apnea

**Figure 8:** Additional ambiguity heatmaps for each near-optimal metric. Results shown for the datasets mammo, compas\_arrest, apnea, and for  $\epsilon$ -level sets defined on loss (1%), AUC (0.5%), and ECE (0.02%).